Observer Quality as a Resource Variable in Quantum Darwinism: Optimal Decoding, ε-Approximate Spectrum Broadcast Structure, and a Central-Spin Worked Example

Alia Wu[1, *]

[1] *Risk Efficacy & Redline Rising*[†]

(Dated: February 18, 2026)

Quantum Darwinism (QD) and Spectrum Broadcast Structure (SBS) formalize how many observers can infer the same pointer value of a system by accessing different fragments of its environment. Most QD analyses treat observers as ideal. We introduce an explicit observer-quality triple $Q_O = (R_O, \Lambda_O, \tau_O)$ encoding access fraction, calibration noise (as a CPTP map), and temporal integration horizon. Replacing conditional i.i.d. record assumptions with an explicit ε-SBS trace-distance approximation, we propagate observer constraints through redundancy/objectivity statements using decoder-level continuity.

Our main results are: (i) Chernoff sample-complexity bounds (upper bounds and achievable exponents) for the number of fragments required to infer a *binary* pointer value under calibration, (ii) a data-processing theorem showing calibration noise cannot increase the quantum Chernoff exponent, and (iii) ε-robust upgrades from ideal SBS to approximate SBS with explicit additive error control.

We provide a worked open-system example (central-spin pure dephasing) computing fragment overlaps, Chernoff exponents, and calibration indices from Hamiltonian couplings and depolarizing readout noise. We also clarify the scope of "local vs collective" decoding claims: for two pure hypotheses, optimal individual strategies can match collective exponents [1], while commonly used *fixed* per-fragment readouts (e.g., repeated Helstrom measurements) can incur a constant-factor penalty. We introduce a coarse decoder-stage label $q_O \in \{q_{\mathrm{D}}, q_{\mathrm{L}}, q_{\mathrm{N}}\}$ (Dot/Linear/Network) mapping observer constraints to memoryless, product-measurement, and collective-decoding regimes. We show that an unmonitored collective decoder can be outperformed by product decoding when coherence reliability falls below a critical threshold (inverted sophistication); the inversion requires observer-side rather than system-side decoherence.

I. INTRODUCTION

Quantum Darwinism (QD) proposes that classical objectivity arises when information about a pointer observable is redundantly encoded in the environment and can be accessed by many observers [2–4]. Spectrum Broadcast Structure (SBS) provides a structural characterization of objective states [5, 6], and strong-QD connects entropic and structural conditions [6, 7].

A recurring modeling gap is that the observer is typically idealized. Yet realistic observers have limited access, imperfect calibration, and finite temporal horizons. There is substantial prior work on non-ideal *environments* (e.g., hazy environments [8]), on the temporal dynamics of information broadcasting [9], on generic emergence of objectivity [10, 11], and on operational approaches emphasizing *accessible* information rather than mutual information [12]. Here we focus on a complementary operational question: given an explicit observer constraint model, what fragment count is sufficient for reliable pointer inference, and how stable are such statements under an explicit ε-approximation to SBS?

Technically, we recast "learning the pointer value" as a binary hypothesis-testing task on fragment registers and use the quantum Chernoff bound [13, 14] to connect redundancy to sample complexity. Many ingredients are standard (Chernoff exponents, data processing, trace-distance continuity), but the contribution is to: (i) package them into an observer-quality parameterization aligned with QD/SBS language, (ii) state explicit theorem hypotheses (access model, calibration model, ε-SBS approximation), and (iii) give a reproducible open-system worked example.

II. SETUP: SBS, ε-SBS, AND OBSERVER QUALITY

Let S be the system and $\mathcal{E} = \mathcal{E}_1 \otimes \cdots \otimes \mathcal{E}_N$ an environment partition. We focus on a pointer variable X taking values in a finite alphabet $\mathcal{X}$.

Definition 1 (Spectrum Broadcast Structure (SBS))**.** A state $\sigma_{S\mathcal{E}}$ has *SBS* with respect to pointer basis $\{|x\rangle\}_{x\in\mathcal{X}}$ if

$$\sigma_{S\mathcal{E}} = \sum_{x\in\mathcal{X}} p_x \, |x\rangle\langle x|_S \otimes \bigotimes_{k=1}^{N} \sigma_{\mathcal{E}_k}^{(x)}, \tag{1}$$

where, for each k, the conditional states $\{\sigma_{\mathcal{E}_k}^{(x)}\}_{x\in\mathcal{X}}$ have mutually orthogonal supports (perfect distinguishability) [5, 6].

Definition 2 (ε-SBS)**.** A state $\rho_{S\mathcal{E}}$ is *ε-SBS* if there exists an SBS state $\sigma_{S\mathcal{E}}$ such that $D_{\mathrm{tr}}(\rho_{S\mathcal{E}}, \sigma_{S\mathcal{E}}) \le \varepsilon$.

* ORCID: 0009-0005-4424-102X

† wut08@nyu.edu

TABLE I. Notation and standing assumptions. Items labeled "(Assumption)" are stated explicitly in Assumption 1 and referenced in theorem hypotheses.

Symbol	Meaning
S	system; pointer basis $\{\|x\rangle\}_{x\in\mathcal{X}}$
$\mathcal{E}=\bigotimes_{k=1}^{N}\mathcal{E}_k$	environment partition into fragments
$X\in\mathcal{X}$	pointer variable; in this paper, theorems focus on $\mathcal{X}=\{0,1\}$ (Assumption)
R_O	access fraction; $m_{\max}=\lfloor R_O N\rfloor$ fragments per episode (Assumption)
Λ_O	per-fragment CPTP calibration/preprocessing map (Assumption)
τ_O	temporal horizon (acquisition/memory time)
$Q(\rho,\sigma)$	quantum Chernoff coefficient $\min_{s\in[0,1]}\mathrm{Tr}[\rho^s\sigma^{1-s}]$
$\xi(\rho,\sigma)$	Chernoff exponent $-\log Q(\rho,\sigma)$
$D_{\mathrm{tr}}(\rho,\sigma)$	trace distance $\frac{1}{2}\|\rho-\sigma\|_1$
Decoder stage	**Operational measurement restriction**
q_{D} (Dot)	single-fragment (memoryless) decoding
q_{L} (Linear)	product (non-entangling) measurements across fragments + classical postprocessing
q_{N} (Network)	collective POVMs on the multi-fragment register

Definition 3 (Observer quality)**.** An observer is specified by a quality triple $Q_O=(R_O,\Lambda_O,\tau_O)$: R_O is an access fraction, Λ_O is a CPTP calibration/preprocessing map applied to each accessed fragment, and τ_O is a temporal horizon (acquisition/memory time).

Assumption 1 (Standing assumptions for theorems)**.** Unless stated otherwise, we adopt the following modeling assumptions.

1. **Binary pointer and equal priors.** The decoding task is $X\in\{0,1\}$ with $p_0=p_1=1/2$.
2. **Witness-experiment product structure.** Conditioned on $X=x$, the accessed fragment register is a product state $\sigma_A^{(x)}=\bigotimes_{k\in A}\sigma_{\mathcal{E}_k}^{(x)}$. (This holds exactly for SBS states and serves as an explicit witness-experiment assumption when working with ε-SBS.)
3. **Independent calibration.** The observer applies the same CPTP map Λ_O independently to each accessed fragment prior to readout, i.e., $\Lambda_O^{\otimes|A|}$.
4. **Access constraint.** In one episode, at most $m_{\max}=\lfloor R_O N\rfloor$ fragments can be accessed.

When $\mathcal{X}=\{0,1\}$, it is useful to define a scalar *single-fragment calibration index* from the Helstrom success probability.

Definition 4 (Binary calibration index)**.** Let ρ_0,ρ_1 be the two conditional states of a single accessed fragment after Λ_O, with equal priors. Define

$$C_O := 1-P_e^\star(\rho_0,\rho_1),$$
$$P_e^\star(\rho_0,\rho_1)=\tfrac{1}{2}\big(1-\tfrac{1}{2}\,\|\rho_0-\rho_1\|_1\big), \qquad (2)$$

where $P_e^\star$ is the Helstrom-optimal Bayes error [15, 16].

Definition 5 (Decoder stage label (three q-states))**.** In addition to the continuous resource triple $Q_O=(R_O,\Lambda_O,\tau_O)$, it is useful to coarse-grain observers into three *decoder regimes*. We introduce a discrete label $q_O\in\{q_{\mathrm{D}},q_{\mathrm{L}},q_{\mathrm{N}}\}$, defined by the admissible measurement class on an m-fragment register: q_{D} (Dot) allows only single-fragment decoding, q_{L} (Linear) allows product (non-entangling) measurements with classical postprocessing, and q_{N} (Network) allows collective POVMs on $\bigotimes_{k\in A}\mathcal{E}_k$. This mirrors the DLN stage coarse-graining in [17], but the present paper is self-contained.[1]

Remark 1 (Finite-resource viewpoint)**.** The fragment-count thresholds below are finite-resource statements and can be read as sample-complexity bounds in quantum hypothesis testing [18–20]. Theorems are stated for a binary pointer; multi-hypothesis extensions are discussed briefly in Remarks where relevant.

[1] The extended preprint version of this paper develops the DLN instantiation in full, including: (i) a proof that SBS conditional independence defines a bipartite factor DAG whose latent node is the pointer variable, (ii) a strict-nesting proof for the decoder classes $\mathsf{Dec}_D\subsetneq\mathsf{Dec}_L\subsetneq\mathsf{Dec}_N$ with a tight, achievable exponent separation (Proposition 3 of the preprint), (iii) a revision-graph formalism governing adaptive transitions between measurement strategies under changing coherence conditions, and (iv) a concrete coherence-gated monitoring protocol. These structural results are independent of the quantitative bounds derived here but provide the graph-theoretic framework in which the decoder-stage classification is naturally situated. The preprint and reproducibility code are archived at https://zenodo.org/records/18610548.

TABLE II. Decoder stage labels, their operational signatures, and correspondence to the DLN stages of Ref. [17].

q_O	DLN stage	DLN representational signature	Operational signature (QD decoding)
q_{D}	Dot	No cross-fragment information retained	Single-fragment / memoryless decoding
q_{L}	Linear	Each fragment processed independently	Product measurements + classical postprocessing
q_{N}	Network	Fragments jointly processed using shared pointer record	Collective decoding (global POVM)

III. CHERNOFF DECODING BOUNDS AND CALIBRATION CONTRACTION

Under Assumption 1, decoding on a fragment set $A \subseteq \{1, \dots, N\}$ is the hypothesis test

$$H_0 : \rho_A^{(0)} := \bigotimes_{k\in A} \Lambda_O\big(\sigma_{\mathcal{E}_k}^{(0)}\big), \tag{3}$$

$$H_1 : \rho_A^{(1)} := \bigotimes_{k\in A} \Lambda_O\big(\sigma_{\mathcal{E}_k}^{(1)}\big). \tag{4}$$

Define the quantum Chernoff coefficient $Q(\rho,\sigma) = \min_{s\in[0,1]} \mathrm{Tr}[\rho^s\sigma^{1-s}]$ and exponent $\xi(\rho,\sigma) = -\log Q(\rho,\sigma)$ [13, 14].

Theorem 1 (Finite-n Chernoff upper bound)**.** *Consider a binary test with equal priors between $H_0 : \rho$ and $H_1 : \sigma$ on a fixed Hilbert space. The Helstrom-optimal Bayes error satisfies*

$$P_e^\star(\rho,\sigma) \le \tfrac{1}{2}\, Q(\rho,\sigma). \tag{5}$$

Definition 6 (Observer-effective Chernoff exponent on a fragment set)**.** For an observer O and fragment set A, define

$$\begin{aligned}\xi_O(A) &:= \xi\big(\rho_A^{(0)}, \rho_A^{(1)}\big) \\ &= \max_{s\in[0,1]} \Bigg(-\sum_{k\in A} \log \mathrm{Tr}\Big[\Lambda_O(\sigma_{\mathcal{E}_k}^{(0)})^s \\ &\qquad \times \Lambda_O(\sigma_{\mathcal{E}_k}^{(1)})^{1-s}\Big]\Bigg). \end{aligned} \tag{6}$$

Proposition 1 (Sufficient access condition for δ-decoding)**.** *Assume Assumption 1. Fix a target $\delta \in (0, \frac{1}{2})$. If there exists a fragment set A with $|A| \le m_{\max} = \lfloor R_O N \rfloor$ such that*

$$\xi_O(A) \ge \log\left(\frac{1}{2\delta}\right), \tag{7}$$

then there exists a (collective) measurement on $\bigotimes_{k\in A} \mathcal{E}_k$ for which $\mathbb{P}(\widehat{X} \ne X) \le \delta$.

Remark 2 (Product vs collective decoding in the sufficiency bound)**.** Proposition 1 is phrased for the optimal measurement on the accessed register. If the observer is restricted to a smaller measurement class (e.g., q_{L} product measurements), then $\xi_O(A)$ is replaced by the corresponding achievable exponent for that class.

Theorem 2 (Calibration degrades Chernoff distinguishability)**.** *Let Λ be a CPTP map and ρ, σ quantum states. For every $s \in [0,1]$,*

$$\mathrm{Tr}\big[\Lambda(\rho)^s \Lambda(\sigma)^{1-s}\big] \;\ge\; \mathrm{Tr}\big[\rho^s\sigma^{1-s}\big]. \tag{8}$$

Equivalently, $\xi\big(\Lambda(\rho), \Lambda(\sigma)\big) \le \xi(\rho,\sigma)$.

IV. HETEROGENEOUS FRAGMENTS AND OPTIMAL ACCESS

QD analyses often assume identical records, but concrete open-system models can produce heterogeneous fragment distinguishabilities. For a given $s \in [0,1]$, define the per-fragment log-overlap

$$\begin{aligned}\ell_k(s) := -\log \mathrm{Tr}\big[&\Lambda_O(\sigma_{\mathcal{E}_k}^{(0)})^s \\ &\times \Lambda_O(\sigma_{\mathcal{E}_k}^{(1)})^{1-s}\big]. \end{aligned} \tag{9}$$

Then for any set A, $\xi_O(A) = \max_{s\in[0,1]} \sum_{k\in A} \ell_k(s)$. The access constraint $|A| \le m_{\max}$ therefore induces a resource-allocation problem.

Remark 3 (When subset selection is trivial)**.** In special cases (e.g., when the conditional fragment states commute for every k, or when $\ell_k(s)$ is s-independent), one can define a genuine "per-fragment Chernoff information" and the optimal subset is obtained by choosing the largest terms. Outside these cases, the optimal subset can depend on the optimizing s and can be genuinely nontrivial.

Proposition 2 (Best-subset selection for pure records)**.** *Assume Assumption 1 and suppose, additionally, that for each k the conditional fragment states are pure. Then $\ell_k(s)$ is s-independent and the optimal exponent over all sets A of size m is obtained by choosing the m fragments with the largest values of ℓ_k.*

V. ε-SBS ROBUSTNESS OF DECISION RULES

Lemma 1 (Decision-theoretic continuity under trace distance)**.** *Let ρ and σ be states on the same Hilbert space. Let* Dec *be any measurement-plus-decision rule producing a classical hypothesis $\widehat{X}$. Then*

$$\begin{aligned}\big|\mathbb{P}_\rho(\widehat{X} \ne X) - \mathbb{P}_\sigma(\widehat{X} \ne X)\big| \\ \le D_{\mathrm{tr}}(\rho,\sigma). \end{aligned} \tag{10}$$

Theorem 3 (ε-robust Chernoff sample complexity)**.** *Assume Assumption 1. Let $\rho_{S\mathcal{E}}$ be ε-SBS with witness $\sigma_{S\mathcal{E}}$. Fix a fragment set A and observer O. If $\delta > \varepsilon$ and*

$$\xi_O(A) \geq \log\left(\frac{1}{2(\delta-\varepsilon)}\right), \tag{11}$$

then there exists a decision rule on A such that $\mathbb{P}_\rho(\widehat{X} \neq X) \leq \delta$.

VI. LOCAL VERSUS COLLECTIVE DECODING: SCOPE AND A USEFUL SPECIAL CASE

Temporal horizons can restrict feasible measurements. A common distinction is between collective measurements on an m-fragment register (which may require quantum memory to preserve coherence during acquisition and decoding) and individual/product measurements (measuring each fragment immediately). The literature on multiple-copy discrimination makes it important to separate (i) what is true for *optimal* product/LOCC strategies and (ii) what is true for *restricted* local readouts.

Proposition 3 (No universal exponent gap for two pure hypotheses)**.** *Let $|\psi_0\rangle$ and $|\psi_1\rangle$ be two pure states with overlap $c = |\langle\psi_0|\psi_1\rangle| \in (0,1)$. For discriminating m copies with equal priors, there exist individual (non-entangling) measurement strategies whose error exponent matches the collective optimum (and adaptive strategies can match the full Helstrom error for every m) [1].*

Remark 4 (A simple fixed individual measurement achieving the collective Chernoff exponent)**.** Projecting each copy onto the basis $\{|\psi_0\rangle, |\psi_0^\perp\rangle\}$ and deciding "1" if any $|\psi_0^\perp\rangle$ outcome occurs yields Bayes error $P_e = \frac{1}{2}c^{2m}$. This achieves the collective Chernoff exponent $-\log(c^2)$ (though not the optimal finite-m prefactor).

Although there is no *unconditional* exponent separation between product and collective measurements for two pure hypotheses, the situation is richer for mixed-state hypotheses or more than two hypotheses, where *strict* exponent separations can persist even for optimal local strategies [21, 22]. In the pure-state binary case, a constant-factor penalty does arise for certain widely used local readouts. One example is repeated application of the *single-copy Helstrom measurement* (the Bayes-optimal measurement for one copy) followed by optimal classical postprocessing.

Corollary 1 (Tight factor-of-two separation for repeated single-copy Helstrom readout on pure records)**.** *Let $|\psi_0\rangle, |\psi_1\rangle$ be pure with overlap $c \in (0,1)$ and equal priors. Consider discriminating m copies under repeated single-copy Helstrom readout followed by optimal classical postprocessing.*

(i) ***Upper bound.*** *For* any *single-copy POVM applied independently to each copy, the Bhattacharyya coefficient of the induced classical outcome distributions satisfies $B \geq c$ [23], so the achievable product-measurement Chernoff exponent is at most $-\log c$ per copy.*

(ii) ***Achievability.*** *The single-copy Helstrom POVM on two pure states with overlap c produces outcome distributions with Bhattacharyya coefficient $B = c$ exactly (since $B = 2\sqrt{P_e^{(1)}(1-P_e^{(1)})} = c$ where $P_e^{(1)} = \frac{1}{2}(1-\sqrt{1-c^2})$). Thus the product-measurement Chernoff exponent* equals *$-\log c$ per copy.*

(iii) ***Gap.*** *Collective decoding achieves the quantum Chernoff exponent $-\log(c^2) = 2(-\log c)$ per copy. Under this fixed local readout, the collective exponent is exactly twice the product exponent: $\xi_{\mathrm{N}}/\xi_{\mathrm{L}} = 2$.*

VII. WORKED PHYSICAL MODEL: CENTRAL-SPIN PURE DEPHASING

We provide a concrete open-system model and compute observer parameters from physical couplings and noise.

A. Model and fragment overlap

Let S be a qubit with pointer basis the eigenbasis of σ_z^S, and $\mathcal{E}$ consist of N qubits. Consider

$$H = \sigma_z^S \otimes \sum_{k=1}^{N} g_k \sigma_z^{(k)}, \tag{12}$$

and initial environment state $|+\rangle^{\otimes N}$. Conditioned on the pointer value x (eigenvalues ± 1 of σ_z^S), fragment k evolves to $|\phi_k^{(x)}(t)\rangle = e^{\mp i g_k t \sigma_z}|+\rangle$, so the overlap is

$$c_k(t) = \left|\langle\phi_k^{(0)}(t)\rangle\, \phi_k^{(1)}(t)\right| = |\cos(2g_k t)|\,. \tag{13}$$

This pure-dephasing model is standard in decoherence theory and appears frequently in QD/SBS analyses of spin environments [6, 24, 25].

B. Chernoff exponent and redundancy

For pure conditional records, the Chernoff coefficient equals the fidelity, so the per-fragment exponent is $-\log c_k(t)^2$. For a set A of accessed qubits,

$$\begin{aligned}\xi(A;t) &= \sum_{k\in A}\left[-\log c_k(t)^2\right] \\ &= \sum_{k\in A}\left[-\log\cos^2(2g_k t)\right].\end{aligned} \tag{14}$$

A sufficient condition for error $\leq \delta$ is $\xi(A;t) \geq \log(1/(2\delta))$ (Proposition 1).

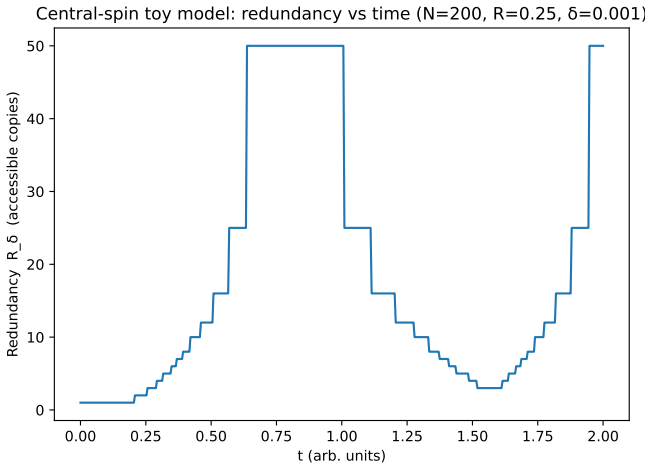

FIG. 1. Central-spin model: redundancy (accessible copies) versus interaction time t for a sampled coupling distribution (uniform around $g_0 = 1$), access fraction $R_O = 0.25$, and target error $\delta = 10^{-3}$. Produced by the repository script `scripts/central_spin_example.py`.

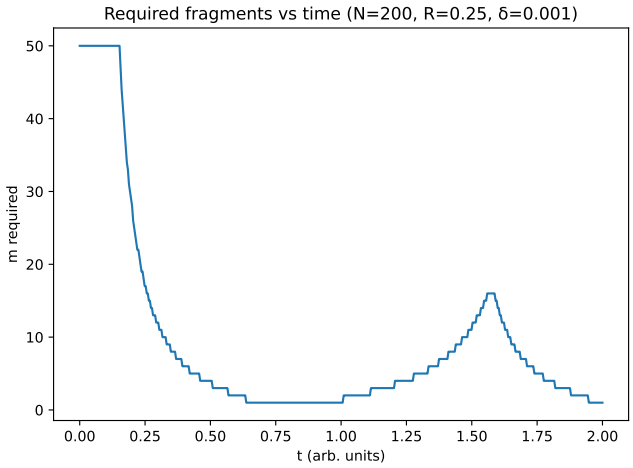

FIG. 2. Same setting as Fig. 1: minimal number of accessed qubits required (under best-subset selection) to achieve target error $\delta = 10^{-3}$ using the Chernoff bound. This figure verifies the qualitative behavior of Proposition 1 in a concrete model.

C. Mapping to (R_O, C_O, τ_O)

Access. If $m_{\max}$ qubits are interceptable per episode out of N, then $R_O = m_{\max}/N$.

Calibration. Suppose the observer's instrument applies a depolarizing channel to each accessed qubit, $\Lambda_p(\rho) = (1-p)\rho + p\frac{\mathbf{1}}{2}$. Depolarization contracts trace distance by factor $(1-p)$ [16]. In the present model, the single-copy Helstrom success probability becomes

$$C_O^{(k)}(t) = \tfrac{1}{2}\big(1 + (1-p)\sqrt{1 - c_k(t)^2}\big) = \tfrac{1}{2}\big(1 + (1-p)|\sin(2g_k t)|\big). \quad (15)$$

Time horizon. Collective decoding across m fragments may require preserving coherence for at least the acquisition time plus decoding time. If t_{meas} is per-qubit acquisition time, a minimal feasibility constraint is $\tau_O \gtrsim m\, t_{\text{meas}}$. More generally, the temporal structure of SBS formation has been studied by Mironowicz, Korbicz, and Horodecki [9], who showed that the broadcasting process can be monitored in time; τ_O parameterizes the observer's temporal window within this process. Pointer stability over the acquisition interval is typically limited by relaxation times (e.g., T_1) [26, 27].

D. Robustness to coupling heterogeneity, noise, and access assumptions

The central-spin toy model is intended as a worked example rather than a claim of universality. To address robustness and interpretation, we report two checks performed by the reproducibility code: (i) varying the coupling distribution (uniform vs Gaussian with matched mean and scale), and (ii) varying depolarizing readout noise p. We also compare an optimistic *best-subset* access model to a conservative *random-access* model in which the observer samples accessible fragments uniformly. Figure 3 summarizes the resulting fragment requirements at fixed interaction time.

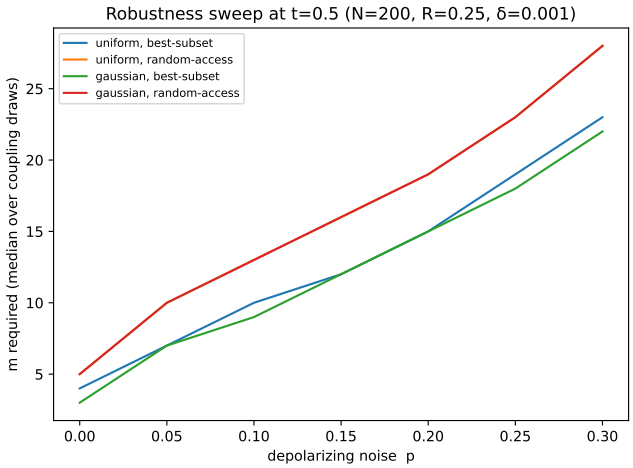

FIG. 3. Robustness check in the central-spin model (Sec. VII). For fixed interaction time $t = 0.5$, we plot the minimal required fragment count (median over coupling draws) as a function of depolarizing noise p. Curves compare coupling distributions (uniform vs Gaussian) and access models (best-subset vs random-access). This quantifies how coupling heterogeneity and readout noise shift the sample-complexity threshold while preserving qualitative behavior.

Remark 5 (Physical implementability of best-subset selection)**.** The best-subset model corresponds to an observer who can preferentially sample fragments with larger distinguishability (e.g., due to spatial proximity or larger

couplings) and/or can postselect which accessible fragments to read out. Many experimental scenarios are closer to random access (e.g., uncontrolled scattering directions). Figure 3 therefore brackets performance between an optimistic "informed" access regime and a conservative "uninformed" regime.

E. Scope and limitations of the central-spin example

The central-spin pure-dephasing model is chosen for analytic tractability and direct connection to SBS formation in spin environments [6, 24]. Several features of this model are not generic:

1. *Pure-state records.* Because the Hamiltonian (12) commutes with σ_z^S, the conditional fragment states remain pure at all times. This saturates the factor-of-two exponent gap (Cor. 1). In models with system–environment entanglement beyond the pointer basis (e.g., spin-boson models with non-commuting coupling, or photon-scattering models with photon loss [28]), fragment records are generically mixed, and the exponent ratio ξ_N/ξ_L lies strictly between 1 and 2 [21].

2. *No relaxation (T_1) processes.* Pure dephasing preserves pointer-basis populations by construction. In systems with relaxation (e.g., spontaneous emission, amplitude damping), the pointer value itself degrades over time, introducing a competition between information encoding rate and pointer decay that is absent here.

3. *No finite-temperature effects.* The initial environment state $|+\rangle^{\otimes N}$ is a pure product state. At finite temperature, the initial environment is mixed, reducing the achievable per-fragment Chernoff exponent and requiring a joint treatment of thermal noise and calibration noise.

4. *No back-action beyond decoherence.* The $[\sigma_z^S, H] = 0$ structure means the system exerts no force on the environment beyond conditional phase kicks. Models with energy exchange (e.g., Jaynes–Cummings or collision models) can produce fragment records whose distinguishability depends on the system's dynamical trajectory, not just its pointer eigenvalue.

Extending the observer-quality framework to these settings requires replacing the analytic overlap formula (13) with numerical Chernoff-coefficient computations, but the formal results (Theorems 1–3) apply without modification.

F. Inverted sophistication: when collective decoding underperforms

The decoder hierarchy $\mathsf{Dec}_L \subsetneq \mathsf{Dec}_N$ (Definition 5) guarantees that the *optimal* collective POVM achieves error no larger than the optimal product measurement. However, if an observer deploys a collective decoder *without monitoring coherence conditions*, decoherence during measurement can cause the collective strategy to underperform product decoding.

Model the observer's coherence reliability as follows. In each episode, with probability f_{coh} coherence is maintained and the collective POVM succeeds (error P_e^{coll}); with probability $1 - f_{\mathrm{coh}}$ coherence fails and the output is uninformative ($P_e = \frac{1}{2}$). The effective error of an unmonitored collective decoder is

$$P_e^{\mathrm{unmon}}(m) = f_{\mathrm{coh}}\, P_e^{\mathrm{coll}}(m) + (1 - f_{\mathrm{coh}})\, \tfrac{1}{2}. \quad (16)$$

For large m, $P_e^{\mathrm{coll}}(m) \to 0$ exponentially, so $P_e^{\mathrm{unmon}} \to (1 - f_{\mathrm{coh}})/2$—a constant floor. Meanwhile, the product decoder's error $P_e^{\mathrm{prod}}(m) = \frac{1}{2}e^{-\xi_L m}$ continues to decrease. For any $f_{\mathrm{coh}} < 1$, there exists a critical fragment count m^* above which product decoding achieves strictly lower error than unmonitored collective decoding.

Equating these two error expressions yields the critical coherence fraction below which inversion occurs at fragment count m:

$$f^*(m) = \frac{P_e^{\mathrm{prod}}(m) - \frac{1}{2}}{P_e^{\mathrm{coll}}(m) - \frac{1}{2}}. \quad (17)$$

Since P_e^{coll} decays faster than P_e^{prod} by the factor-of-two exponent gap (Corollary 1), $f^*(m) \to 1$ as $m \to \infty$: the coherence margin required for unmonitored collective decoding to remain competitive shrinks to zero.

Figure 4 illustrates this for the central-spin model. The left panel shows that at $f_{\mathrm{coh}} = 0.9$ the unmonitored collective error saturates at a floor of 0.05, while the product decoder continues to improve. The right panel shows $1 - f^*$ versus m: the coherence margin collapses exponentially, meaning that even 99.99% coherence reliability becomes insufficient at large m.

This result is robust across decoherence models:

1. *Continuous exponent degradation* (replacing the binary model with $P_e = \frac{1}{2}e^{-f_{\mathrm{coh}}\,\xi_N m}$): inversion occurs at a model-independent threshold $f^* = \frac{1}{2}$.

2. *System-side depolarization* (fragment states themselves become mixed): both decoders degrade symmetrically and no inversion occurs; the collective advantage persists for all $f_{\mathrm{coh}} > 0$.

The physical conclusion is that inverted sophistication requires *observer-side* decoherence (apparatus-level coherence failure), not *system-side* decoherence (noise on the fragment states themselves).

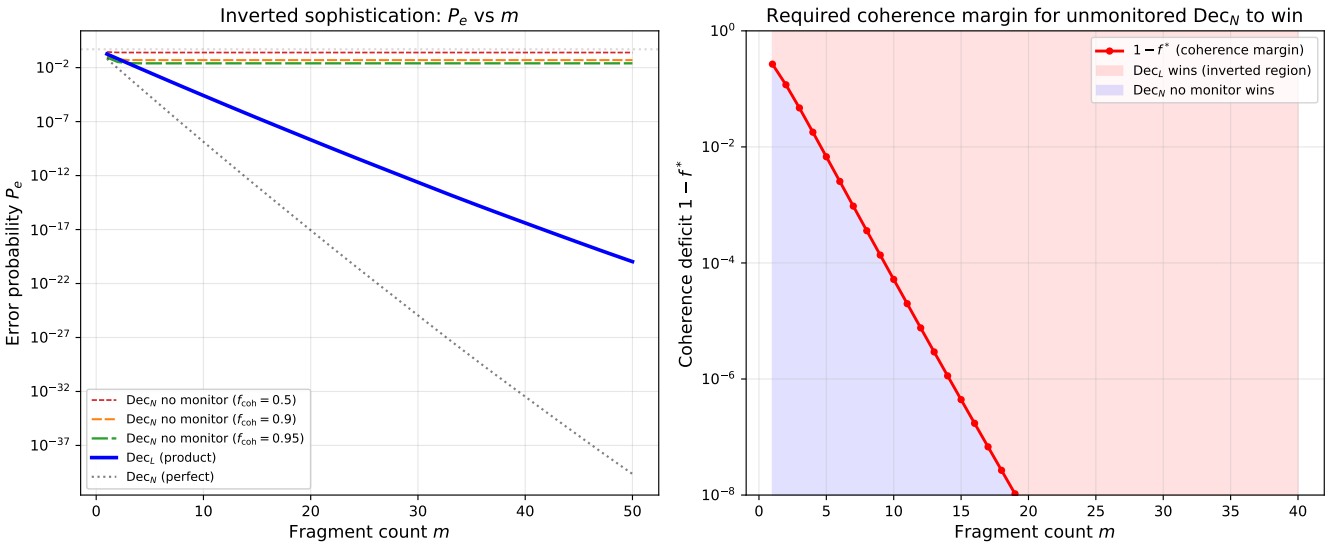

FIG. 4. Inverted sophistication in the central-spin model. The crossover is driven by the factor-of-two exponent gap between product and collective decoding (Cor. 1): when coherence monitoring fails, the collective decoder's exponent advantage becomes a liability. *Left:* Error probability vs. fragment count m for product decoding (Dec_L, solid blue) and unmonitored collective decoding (Dec_N, dashed) at three coherence fractions. At $f_{\mathrm{coh}} < 1$, the unmonitored collective error saturates at $(1 - f_{\mathrm{coh}})/2$ while Dec_L continues to improve. *Right:* Required coherence margin $1 - f^*$ vs. m (log scale). Above the curve (pink region), the product decoder achieves lower error; below (blue region), unmonitored collective decoding wins. The margin collapses exponentially with m.

VIII. CONCLUSION

Explicit observer-quality parameterization yields decoder-level, ε-robust sample-complexity bounds for QD/SBS. Calibration is a provable contraction of the Chernoff exponent (Theorem 2), and ε-SBS approximations propagate to operational error bounds with explicit additive control (Theorem 3). The central-spin example demonstrates how these quantities can be computed from Hamiltonian couplings and readout noise, and provides robustness checks against coupling heterogeneity and access assumptions. Claims about local-versus-collective decoding must be stated with care: for two pure hypotheses, individual strategies can match collective exponents [1], while additional restrictions (e.g., repeated single-copy Helstrom readout) can impose a constant-factor penalty (Cor. 1). Moreover, an unmonitored collective decoder can be strictly outperformed by a product decoder when coherence reliability drops below a critical threshold that shrinks exponentially with fragment count; this inverted sophistication requires observer-side rather than system-side decoherence (Sec. VII F).

The present results are restricted to binary pointer alphabets and pure-state fragment records; mixed-state records generically reduce the collective/product exponent ratio below 2, and multi-hypothesis extensions require modified Chernoff bounds. The binary decoherence model (Model A) gives the strongest inversion threshold ($f^* \to 1$); the continuous model (Model B, $f^* = 1/2$ independently of m) may be more representative in many settings.

The observer-quality triple (R_O, Λ_O, τ_O) and the resulting exponent bounds are defined in terms of experimentally accessible quantities—access fraction, readout noise channel, and integration time—making them directly applicable to photonic quantum Darwinism experiments [28, 29] and other platforms where fragment-level measurement statistics are available [30].

ACKNOWLEDGMENTS

All numerical code and figure-generation scripts for this work are publicly available at https://github.com/aliawu08/dln-observer-quality-quantum-darwinism and archived at Zenodo [31].

Appendix A: Proofs and standard lemmas

This appendix provides complete derivations for the results used in the main text.

1. Proof of Theorem 1

For equal priors, the minimum achievable Bayes error is

$$P_e^\star(\rho,\sigma) = \tfrac{1}{2}\left(1 - \tfrac{1}{2}\|\rho-\sigma\|_1\right). \tag{A1}$$

The finite-n quantum Chernoff bound of Ref. [13] implies that for all states ρ, σ,

$$\begin{aligned} P_e^\star(\rho,\sigma) &\le \tfrac{1}{2}\min_{s\in[0,1]} \mathrm{Tr}[\rho^s\sigma^{1-s}] \\ &= \tfrac{1}{2}\,Q(\rho,\sigma), \end{aligned} \tag{A2}$$

which is Eq. (5).

2. Proof of Proposition 1

By Theorem 1 applied to $(\rho_A^{(0)}, \rho_A^{(1)})$,

$$P_e^\star\big(\rho_A^{(0)}, \rho_A^{(1)}\big) \le \tfrac{1}{2}\exp\big(-\xi_O(A)\big). \tag{A3}$$

If Eq. (7) holds, then $\frac{1}{2}\exp\big(-\xi_O(A)\big) \le \delta$. Thus the optimal decision rule (the Helstrom measurement on the $|A|$-fragment register) achieves error at most δ.

3. Proof of Theorem 2

Fix $s \in (0,1)$. Define the Petz-Rényi divergence [32]

$$D_s(\rho\|\sigma) = \frac{1}{s-1}\log\,\mathrm{Tr}[\rho^s\sigma^{1-s}]. \tag{A4}$$

For $s \in (0,1)$, data processing holds under CPTP maps [18, 32, 33]: $D_s(\Lambda(\rho)\|\Lambda(\sigma)) \le D_s(\rho\|\sigma)$. Multiplying both sides by $(s-1) < 0$ reverses the inequality and yields

$$\log\,\mathrm{Tr}[\Lambda(\rho)^s\Lambda(\sigma)^{1-s}] \ge \log\,\mathrm{Tr}[\rho^s\sigma^{1-s}], \tag{A5}$$

which implies Eq. (8). Taking the minimum over $s \in [0,1]$ gives $Q(\Lambda(\rho),\Lambda(\sigma)) \ge Q(\rho,\sigma)$, and therefore $\xi(\Lambda(\rho),\Lambda(\sigma)) \le \xi(\rho,\sigma)$.

4. Proof of Lemma 1

Any measurement-plus-decision rule is a CPTP map $\mathcal{M}$ from quantum states to a classical probability distribution over outcomes. For classical distributions, the trace distance equals total variation distance. By data processing for trace distance under CPTP maps [16],

$$D_{\mathrm{tr}}\big(\mathcal{M}(\rho),\mathcal{M}(\sigma)\big) \le D_{\mathrm{tr}}(\rho,\sigma). \tag{A6}$$

For any event E in the classical output (in particular the event $\{\widehat{X} \ne X\}$), the difference in event probabilities is bounded by total variation distance. This yields Eq. (10).

5. Proof of Theorem 3

Let $\sigma_{S\mathcal{E}}$ be an SBS witness state with $D_{\mathrm{tr}}(\rho_{S\mathcal{E}},\sigma_{S\mathcal{E}}) \le \varepsilon$. By Proposition 1 applied to $\sigma_{S\mathcal{E}}$, if Eq. (11) holds then there exists a decision rule on A whose error under $\sigma_{S\mathcal{E}}$ is at most $(\delta-\varepsilon)$. Applying Lemma 1 to the induced two-outcome classical distributions (error vs success) gives

$$\begin{aligned} \mathbb{P}_\rho(\widehat{X} \ne X) &\le \mathbb{P}_\sigma(\widehat{X} \ne X) + D_{\mathrm{tr}}(\rho_{S\mathcal{E}},\sigma_{S\mathcal{E}}) \\ &\le (\delta-\varepsilon) + \varepsilon = \delta. \end{aligned} \tag{A7}$$

[1] A. Acín, E. Bagan, M. Baig, L. Masanes, and R. Muñoz-Tapia, Physical Review A **71**, 032338 (2005), arXiv:quant-ph/0410097.
[2] H. Ollivier, D. Poulin, and W. H. Zurek, Physical Review Letters **93**, 220401 (2004), arXiv:quant-ph/0307229.
[3] W. H. Zurek, Nature Physics **5**, 181 (2009).
[4] R. Blume-Kohout and W. H. Zurek, Physical Review A **73**, 062310 (2006).
[5] R. Horodecki, J. K. Korbicz, and P. Horodecki, Physical Review A **91**, 032122 (2015).
[6] J. K. Korbicz, Quantum **5**, 571 (2021), arXiv:2007.04276.
[7] T. P. Le and A. Olaya-Castro, Physical Review Letters **122**, 010403 (2019).
[8] M. Zwolak, H. T. Quan, and W. H. Zurek, Physical Review Letters **103**, 110402 (2009).
[9] P. A. Mironowicz, J. K. Korbicz, and P. Horodecki, Physical Review Letters **118**, 150501 (2017), arXiv:1607.02478.
[10] F. G. S. L. Brandão, M. Piani, and P. Horodecki, Nature Communications **6**, 7908 (2015).
[11] P. A. Knott, T. Tufarelli, M. Piani, and G. Adesso, Physical Review Letters **121**, 160401 (2018), arXiv:1802.05719.
[12] A. Touil, B. Yan, D. Girolami, S. Deffner, and W. H. Zurek, Physical Review Letters **128**, 010401 (2022), arXiv:2107.00035.
[13] K. M. R. Audenaert, M. Nussbaum, A. Szkoła, and F. Verstraete, Physical Review Letters **98**, 160501 (2007), arXiv:quant-ph/0610027.
[14] M. Nussbaum and A. Szkoła, The Annals of Statistics **37**, 1040 (2009), arXiv:quant-ph/0607216.
[15] C. W. Helstrom, *Quantum Detection and Estimation Theory* (Academic Press, 1976).
[16] J. Watrous, *The Theory of Quantum Information* (Cambridge University Press, 2018).
[17] A. Wu, bioRxiv 10.64898/2026.02.01.703168 (2026).
[18] M. Tomamichel, *Quantum Information Processing with Finite Resources: Mathematical Foundations*, SpringerBriefs in Mathematical Physics, Vol. 5 (Springer, 2016).
[19] K. M. R. Audenaert, M. Mosonyi, and F. Verstraete, Journal of Mathematical Physics **53**, 122205 (2012),

arXiv:1204.0711 [quant-ph].
[20] H.-C. Cheng, N. Datta, N. Liu, T. Nuradha, R. Salzmann, and M. M. Wilde, npj Quantum Information **11**, 94 (2025), arXiv:2403.17868.
[21] J. Calsamiglia, J. I. de Vicente, R. Muñoz-Tapia, and E. Bagan, Physical Review Letters **105**, 080504 (2010), arXiv:1005.1692.
[22] M. Owari and M. Hayashi, New Journal of Physics **10**, 013006 (2008), arXiv:0708.3154.
[23] C. A. Fuchs and C. M. Caves, Physical Review Letters **73**, 3047 (1994).
[24] K. Roszak and J. K. Korbicz, Physical Review A **100**, 062127 (2019).
[25] M. Zwolak, C. J. Riedel, and W. H. Zurek, Scientific Reports **6**, 25277 (2016).
[26] H.-P. Breuer and F. Petruccione, *The Theory of Open Quantum Systems* (Oxford University Press, 2002).
[27] M. Schlosshauer, *Decoherence and the Quantum-to-Classical Transition* (Springer, 2007).
[28] C. J. Riedel and W. H. Zurek, Physical Review Letters **105**, 020404 (2010).
[29] M. A. Ciampini, G. Pinna, P. Mataloni, and M. Paternostro, Physical Review A **98**, 020101 (2018).
[30] T. K. Unden, D. Louber, N. Balzarotti, M. Maile, and F. Jelezko, Physical Review Letters **123**, 140402 (2019).
[31] A. Wu, Observer quality as a resource variable in quantum darwinism — reproducibility code and data (2026).
[32] D. Petz, Reports on Mathematical Physics **23**, 57 (1986).
[33] M. Mosonyi and T. Ogawa, Communications in Mathematical Physics **334**, 1617 (2015).